Expression and glycoengineering of functionally active heteromultimeric IgM in plants

Andreas Loos[a], Clemens Gruber[b], Friedrich Altmann[b], Ulrich Mehofer[a], Frank Hensel[c], Melanie Grandits[d], Chris Oostenbrink[d], Gerhard Stadlmayr[b], Paul G. Furtmüller[b], and Herta Steinkellner[a,1]

[a]Department of Applied Genetics and Cell Biology, University of Natural Resources and Life Sciences, 1190 Vienna, Austria; [b]Department of Chemistry, University of Natural Resources and Life Sciences, 1190 Vienna, Austria; [c]Patrys GmbH, 97076 Würzburg, Germany; and [d]Institute of Molecular Modelling and Simulation, University of Natural Resources and Life Sciences, 1190 Vienna, Austria

Edited by Charles J. Arntzen, Arizona State University, Tempe, AZ, and approved February 25, 2014 (received for review November 13, 2013)

IgM antibodies are an important player of the human's innate defense mechanisms and increasingly have gained interest as therapeutics. Although the expression of IgM antibodies in mammalian cell culture is established, this approach remains costly and alternative methods have not been developed yet. Plants have a proven record for the production of therapeutically relevant recombinant proteins. However, whether they are able to express proteins like IgM antibodies, which range among the most complex human proteins, remains unknown so far. Here we report the *in planta* generation of the functionally active monoclonal antitumor IgM PAT-SM6 (SM6). SM6 efficiently accumulates in plant leaves and assembles correctly into heterooligomers (pentamers and hexamers). Detailed glycosylation analysis exhibited complex and oligomannosidic N-glycans in a site-specific manner on human-serum IgM and on plant- and human-cell-line–produced SM6. Moreover, extensive *in planta* glycoengineering allowed the generation of SM6 decorated with sialylated human-type oligosaccharides, comparable to plasma-derived IgM. A glycosylated model of pentameric IgM exhibits different accessibility of the glycosylation sites, explaining site-specific glycosylation. Biochemical and biophysical properties and importantly biological activities of plant-derived SM6 glycoforms are comparable to the human-cell–derived counterparts. The *in planta* generation of one of the most complex human proteins opens new pathways toward the production of difficult-to-express proteins for pharmaceutical applications. Moreover, the generation of IgMs with a controlled glycosylation pattern allows the study of the so far unknown contribution of sugar moieties to the function of IgMs.

recombinant biopharmaceuticals | N-glycosylation

IgMs form the first class of antibodies produced during a primary antibody response. Apart from their high avidity and agglutination efficiency, IgMs are exceptionally good in complement activation and germline-encoded native IgM plays an important role in defense against aberrant cells (1). Thus, monoclonal IgM antibodies have increasingly gained interest for the treatment of various diseases (2–4). However, despite the recognized relevance for pharmaceutical applications the (recombinant) production has long been considered a challenge (5, 6). This is mainly due to the large size and extensive co- and posttranslational modifications, which rank IgMs among the most complex human proteins known. In human serum, IgMs circulate mainly as ~950 kDa pentamers consisting of 10 heavy, 10 light, and 1 joining chain (~95%), but also as ~1,150 kDa hexamers (~5%; 12 heavy and 12 light chains). Roughly 10% of the molecular weight is made up by N-glycans, which are attached to 5 conserved N-glycosylation sites within the constant domains of each heavy chain. Although it is well demonstrated that correct assembly of the 21 (or 24, depending on the oligomerization status) polypeptides is a prerequisite for the functionality of IgMs (7), the impact of glycosylation is largely unknown. However, results from clinical studies, particularly on IgGs, indicate that carbohydrates play a structural and functional role for all immunoglobulins (8–10).

Intensive efforts over the last years have enabled the production of functionally active IgMs in mammalian cell culture at reasonably high levels (g/L) (5) for clinical applications (3, 4). However, labor-intensive production and, as a consequence, high costs of recombinant IgMs prevented their widespread use. Moreover, heterogeneous and improper N-glycosylation of hybridoma- or cell-culture–produced IgMs might hamper clinical success and impede the investigation of the impact of this important posttranslational modification. These issues can be addressed by using plants as production platform (11). Correctly assembled mammalian proteins like IgGs have been expressed in plants at a high level (12); however, whether plants can also correctly fold and assemble proteins as complex as IgMs is currently unknown. Another important aspect is the specific glycosylation characteristics of plants. Although mammalian cells usually generate proteins with a mixture of glycoforms that are neither identical to the human profile nor optimized for efficacy (13), plants normally produce proteins with a largely homogeneous glycosylation profile. Moreover, plants are amenable to glycoengineering approaches and tolerate the synthesis of human-like N-glycans without obvious negative effects (11). This strategy has been extensively applied for the production of

Significance

IgM antibodies are increasingly gaining interest as therapeutics; however, knowledge about this antibody class is scarce. Specifically the impact of N-glycans on the functional mechanism of this heavily glycosylated molecule is entirely unknown. To address this issue we produced different IgM glycoforms in plants and characterized them. Moreover, we present a computer model that explains the characteristic N-glycosylation pattern of IgMs. With the successful *in planta* generation of recombinant IgMs largely resembling the plasma-derived orthologue, we offer an efficient alternative to mammalian cell-based expression systems. IgMs with targeted glycoengineered N-glycans now enable detailed structure–function studies and will lead to the production of IgMs with optimized in vivo activities.

Author contributions: A.L., F.A., F.H., C.O., P.G.F., and H.S. designed research; A.L., C.G., U.M., F.H., M.G., and G.S. performed research; A.L., C.G., F.A., U.M., F.H., M.G., C.O., G.S., P.G.F., and H.S. analyzed data; and A.L., F.A., F.H., M.G., and H.S. wrote the paper.

Conflict of interest statement: F.H. is an employee of Patrys GmbH, a wholly owned subsidiary of Patrys Limited, which holds the rights of the described IgM.

This article is a PNAS Direct Submission.

Freely available online through the PNAS open access option.

Data deposition: The sequence reported in this paper has been deposited in the GenBank database (accession no. NP_653247.1). The HC and LC sequences are available in the *SI Appendix*.

See Commentary on page 6124.

[1]To whom correspondence should be addressed. E-mail: herta.steinkellner@boku.ac.at.

This article contains supporting information online at www.pnas.org/lookup/suppl/doi:10.1073/pnas.1320544111/-/DCSupplemental.

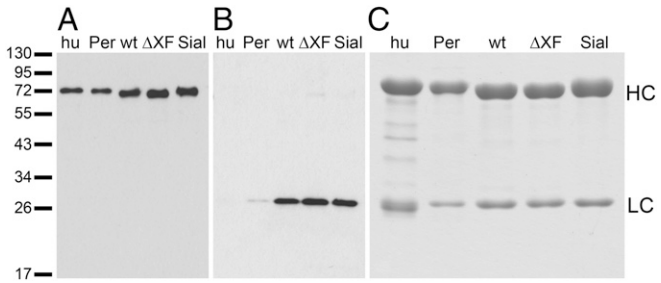

Fig. 1. SM6 glycoforms are equally well expressed in *N. benthamiana* leaves and can be purified by protein A chromatography. (*A* and *B*) Immunoblotting of crude extracts of infiltrated leaves (corresponding to 40 μg leaf material per lane) using antibodies against IgM HC (*A*) and LC (*B*). Human-serum IgM (hu) and PER.C6-produced $SM6_{PER}$ (Per) were used as control (5 ng each). Deducing from the band intensities, a clearly higher ratio of LC to HC is present in the crude plant extract than in the purified human-serum IgM or $SM6_{PER}$. This excess of LC is not present after purification. (*C*) Coomassie-stained SDS-polyacrylamide gel containing purified SM6 and human-serum–derived IgM (5 μg each). Human-serum–derived IgM (hu) and $SM6_{PER}$ (Per) served as controls for plant-produced glycoforms [$SM6_{wt}$ (wt), $SM6_{\Delta XF}$ (ΔXF), and $SM6_{sia}$ (Sial)]. Marker sizes are given in kDa.

monoclonal IgG antibodies (14), where different glycosylation profiles confer strongly altered biological activities (15–18). Although the functioning of IgG has been studied intensively over the last decade, knowledge about IgMs (i.e., assembly, functional activities, and the impact of glycosylation on the function) is lagging behind. A source of different, yet homogenous IgM glycoforms is needed to investigate the effect of glycosylation on the biological properties.

In this study, we sought to explore the *Nicotiana-benthamiana*–based transient expression system (12) for the generation of different IgM glycoforms. As model antibody we used the anticancer IgM PAT-SM6 (SM6; 19, 20), which is proprietary to Patrys Limited. Expression vectors were generated to transiently produce heavy, light, and joining chain (HC, LC, and JC) of SM6 in *N. benthamiana* WT and ΔXT/FT, a mutant lacking plant-specific glycosylation (21), or in lines conferring human-type N-glycosylation. SM6 accumulated in leaves and was successfully purified via protein A. Its folding, its N-glycosylation in a site-directed manner, and its antigen-binding properties were assessed.

Results

SM6 Is Efficiently Expressed in *N. Benthamiana*. We intended to generate three glycoforms of SM6 ($SM6_{wt}$, $SM6_{\Delta XF}$, and $SM6_{sia}$) in *N. benthamiana* by delivering the respective SM6 expression constructs (heavy, light, and joining chain) to WT plants ($SM6_{wt}$), to the glycosylation mutant ΔXT/FT ($SM6_{\Delta XF}$; ref. 21) and by coexpressing the genes necessary for *in planta* sialylation (11) in ΔXT/FT plants ($SM6_{sia}$). IgM expression was monitored by immunoblotting. Already 2–3 d postinfiltration (dpi) specific signals for IgM heavy and light chain were visible (Fig. 1 *A* and *B*). Light chain signals were stronger for crude leaf extracts than for purified IgM (human-serum IgM and $SM6_{PER}$ with a ~1:1 ratio of HC to LC), where a longer exposure was needed to see a signal (Fig. S1). Most likely, this was due to an excess of light chain over heavy chain in the crude extract. Total soluble protein from infiltrated leaves was collected 3–4 dpi and SM6 was subsequently purified by protein A affinity chromatography. This is possible for IgMs containing VH3 domains. SDS-PAGE and Coomassie staining (Fig. 1*C*) exhibited the presence of two strong bands with the expected size for IgM heavy and light chain (75 and 25 kDa, respectively). Overall, the results demonstrate high purity of the plant-derived IgM. IgM levels were quantified after purification and reached up to 84 μg purified IgM per gram of infiltrated leaf.

Glycosite-Specific Glycosylation of Human-Cell–Derived IgM. Human-serum IgM contains five N-glycosylation sites (GS) in the constant region of the heavy chain (GS1–5; Asn171, Asn332, Asn395, Asn402, and Asn563) (22). Previous data from total glycan release experiments showed the presence of complex and oligomannosidic N-glycans (22). Here we set out to determine the glycosylation status of human-serum–derived IgM in a site-specific manner. Liquid chromatography-electrospray ionization-mass spectrometry (LC-ESI-MS) (Fig. 2) exhibited the presence of mainly sialylated complex-type N-glycans on the three N-terminally located GS1–3 (i.e., Asn171, Asn332, and Asn395). Overall two dominant species, monosialylated and fucosylated ANaF and ANaFbi, were present (Table 1 and Fig. 2). In contrast, the C-terminally

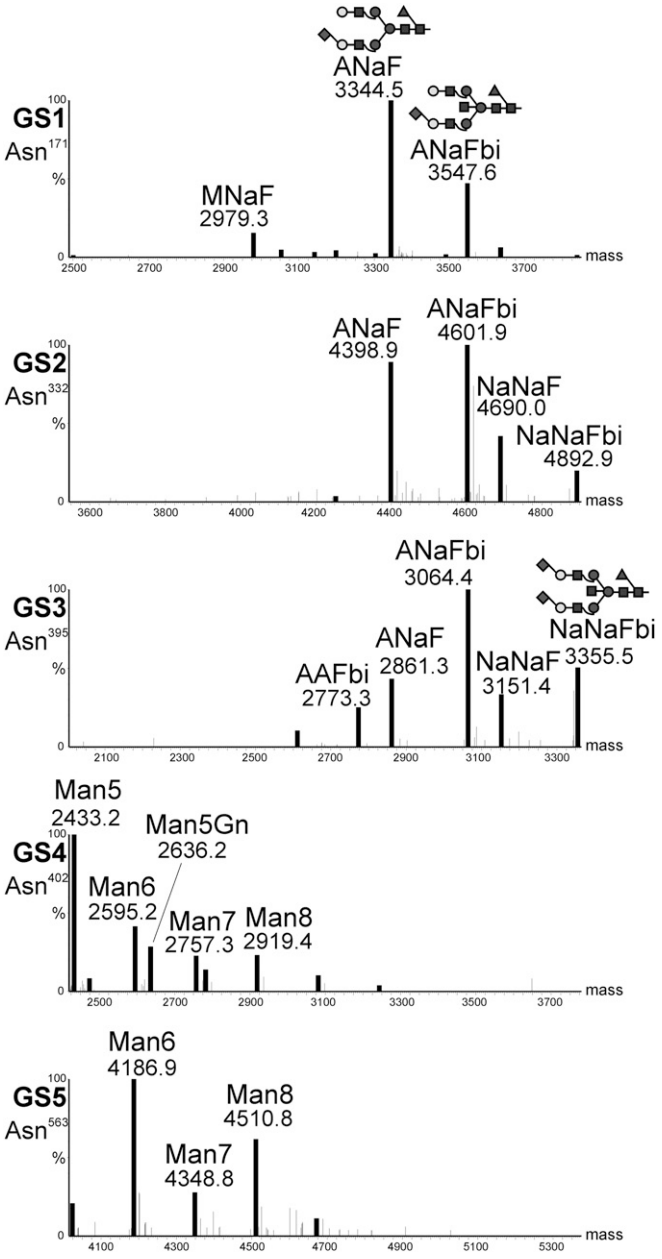

Fig. 2. N-glycosylation profile of human-serum–derived IgM. Mass spectra were generated by LC-ESI-MS of glycopeptides obtained upon trypsin or trypsin/GluC digestion. Profiles of all five HC glycosylation sites are shown. Peaks are labeled in accordance with the ProGlycAn system (www.proglycan.com). Major glycoforms are shown as illustrations.

Table 1. Relative abundance in percentage of major glycostructures detected on human-serum IgM and SM6 produced in different expression hosts

	GS1-3					GS4-5				
Structure	IgM_{hs}	$SM6_{PER}$	$SM6_{wt}$	$SM6_{\Delta XF}$	$SM6_{sia}$	IgM_{hs}	$SM6_{PER}$	$SM6_{wt}$	$SM6_{\Delta XF}$	$SM6_{sia}$
GnGn				52	15					
GnGnF				11						
MGnXF			6							
GnGnXF			60							
MNa					16					
GnAF		7								
AAF		10								
ANa					7					
ANaF	35	30								
ANaFbi	33									
NaNa					17					
NaNaF	10									
NaNaFbi	8									
ANaF+F		10								
∑ other complex	13	29	10	9	13		4	4	4	2
∑ oligoman	1	14	24	29	32	100	96	96	96	98

IgM_{hs}: human-serum–derived IgM; ∑ other complex: sum of glycoforms present at levels below 5%; ∑ oligoman: oligomannosidic and hybrid glycans. The glycan structures are assigned using the ProGlycAn nomenclature (www.proglycan.com).

located GS4 and GS5 (Asn402, Asn563) carry oligomannosidic structures (Fig. 2). Altogether, our analyses largely confirmed the conclusions drawn from a previous study (22). Deviating from that study, which suggested incomplete occupation of GS5 (22), our analyses exhibited full glycosylation of this site (Fig. S2).

As a next step the glycosylation profile of SM6 produced in the human PER.C6 cell line ($SM6_{PER}$) was determined (5). In general, the glycosylation pattern largely resembled that of human-serum–derived IgM: the three N-terminal glycosylation sites are occupied by complex-type N-glycans and the two C-terminal sites carried oligomannosidic structures. However, differences in the type of complex N-glycans were seen compared with human-serum–derived IgMs. Although the monosialylated glycan ANaF emerged as the main glycan structure in both samples (Table 1), $SM6_{PER}$ showed a larger number of complex N-glycan species. Other differences are the presence of difucosylated glycans (i.e., ANaF+F) and the lack of bisected structures (N-acetylglucosamine attached in β-1,4-position to the innermost mannose residue) in $SM6_{PER}$.

Glycosylation Pattern of Plant-Produced SM6 Resembles the Human Counterpart. Glycosylation profiling of SM6 produced in WT plants ($SM6_{wt}$) showed the same distribution of complex and oligomannosidic N-glycans as for serum-derived IgM and $SM6_{PER}$: the N-terminally located GS1–3 were mainly decorated with complex type N-glycans and the C-terminal GS4 and GS5 with oligomannosidic structures. However, in contrast to the human-cell–derived IgMs, GS1–3 carried a single dominant glycan species that lacked galactose and sialic acid residues, but bore plant-typical xylose and fucose (i.e., GnGnXF; Table 1). Initial expression of $SM6_{wt}$ (without coexpression of GnTII) showed roughly 50% of complex glycans having one truncated glycan arm ending with a mannose residue (e.g., MGnXF). Such incompletely processed structures were not detected in human-cell–derived $SM6_{PER}$. Upon coexpression of the human glycosyltransferase GnTII (23), which is responsible for elongating the truncated arm with N-acetylglucosamine residues, we could increase the amount of glycans with fully processed arms (i.e., GnGnFX; Table 1). Thus, GnTII was coexpressed in all experiments.

Using ΔXT/FT plants (21) as expression hosts resulted in the production of $SM6_{\Delta XF}$ carrying oligomannosidic N-glycans on GS4 and GS5, and human-type complex GnGn structures lacking plant-specific xylose and fucose residues at GS1–3. Notably, the glycosylation profiles of $SM6_{\Delta XF}$ GS1–3 are largely homogeneous showing GnGn as the single major N-glycan species (Table 1). To mimic the human N-glycosylation profile we coexpressed the human genes required for *in planta* protein sialylation (24) together with SM6 ($SM6_{sia}$). This resulted in the synthesis of mono- and disialylated glycans on GS1–3 (Table 1). GS4 and GS5 were unaffected and decorated with oligomannosidic structures as in $SM6_{wt}$ and $SM6_{\Delta XF}$.

Plant Cells Express Properly Assembled SM6. To determine the oligomerization status of plant-derived SM6 nonreducing gradient polyacrylamide gels were used as separation matrix. As controls $SM6_{PER}$ consisting mainly of pentamers and $SM6_{PER*}$, a variant without JC consisting of pentamers and hexamers, were included. Purified, plant-derived IgMs exhibited a similar banding

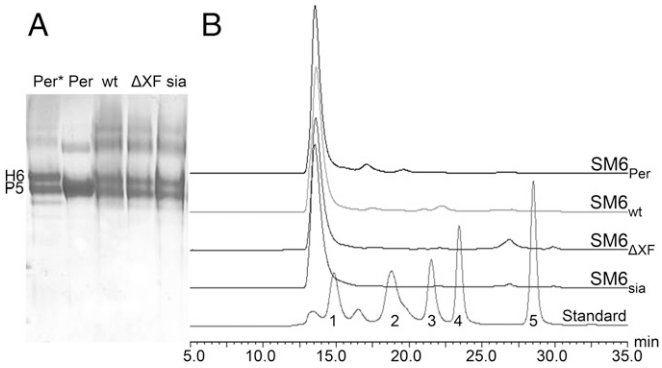

Fig. 3. Plant-derived SM6 glycoforms are properly assembled. (*A*) Evaluation of SM6 oligomerization status by Coomassie-stained gradient PAGE. SM6 produced in PER.C6 cells without JC, containing hexamers and pentamers (Per*; 5); $SM6_{Per}$ (with JC) containing mainly pentamers (Per; 5); $SM6_{wt}$ (wt), $SM6_{\Delta XF}$ (ΔXF), and $SM6_{sia}$ (sia); hexamers (H6) and pentamers (P5) are indicated. In plants, roughly 50:50 hexamers and pentamers are present. (*B*) SEC-HPLC analysis. All tested SM6 batches show a similar size distribution with a single peak at the size of penta/hexameric IgM. Standard sizes are 670, 158, 44, 17, and 1.35 kDa.

pattern as these controls (Fig. 3*A*), with a higher proportion of hexamers in the plant-produced IgMs. In addition, size exclusion chromatography profiles of PER.C6- and plant-derived SM6 were virtually identical confirming the correct oligomerization of the plant-derived IgM (Fig. 3*B*). Electronic circular dichroism (ECD) spectroscopy was applied to compare the secondary structure of SM6 from different sources. The ECD spectra of both plant-produced and human-cell–derived IgM ($SM6_{PER}$) (Fig. 4) are characteristic of a protein composed primarily of β-sheets with a maximum band at 194 nm and a minimum band at 218 nm. Very little difference was observed between the three plant-produced glycoforms. If conformational changes did occur, they must have been very localized and minimal. The distinct spectrum of $SM6_{PER}$ can be explained mainly by different concentrations due to inaccuracies in the protein quantification method and to a minor extent by marginal differences in the secondary structure.

Plant-Derived SM6 Glycoforms Exhibit Functional Integrity. Binding of SM6 to antigen on the surface of human lung carcinoma cells (A549) was assessed by fluorescence-activated cell sorting analysis (Fig. 5). Plant-produced SM6 glycoforms ($SM6_{wt}$, $SM6_{\Delta XF}$, or $SM6_{sia}$) showed virtually identical antigen-binding properties and similar binding as $SM6_{PER}$ (Fig. 5), thereby indicating functional integrity of the different IgM variants. Whether the differences between plant-produced IgM and $SM6_{PER}$ observed in ECD spectroscopy and flow cytometry were caused by the different expression systems (plant versus human cells) or resulted from variations in the purification procedure is currently not known.

SM6 Model Suggests Site-Specific Glycosylation due to Differential Accessibility. One peculiarity of IgM is the distinction between complex (GS1–3) and oligomannosidic (GS4 and GS5) glycosylation sites. Although occasionally observed in nature (e.g., 9, 25) the reasons for the dramatic shift of glycosylation within a single molecule have not been fully elucidated; however, accessibility of N-glycosylation sites might play an important role (26, 27). To investigate factors influencing such processes a computer model of SM6 was generated (Fig. 6) based on previously published structural information (28). Into this model complex glycans (NaNa) for GS1–3 and oligomannosidic glycans (Man8) for GS4 and GS5 were inserted. The model shows that the complex glycans (blue/red) extend into the surrounding space whereas the oligomannosidic glycans (orange/red) are directed toward the inside of the IgM molecule. These data suggest that glycans on GS4 and GS5 are probably inaccessible for some N-glycosylation enzymes during the transport of the assembled protein through the Golgi. Notably, it seems that inaccessibility is mainly restricted to late Golgi acting enzymes, as Man5–Man7 oligomannosidic structures are generated in endoplasmic reticulum and early Golgi compartments.

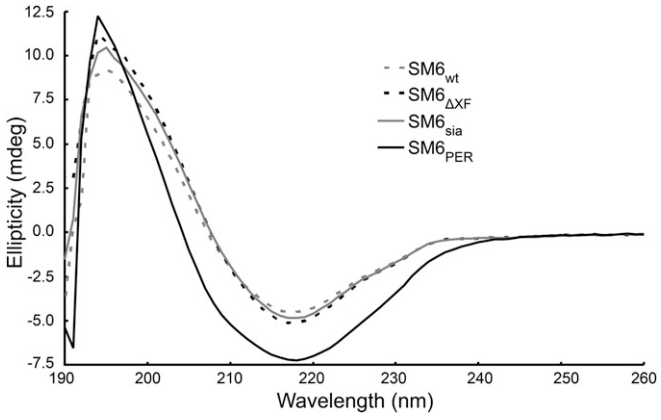

Fig. 4. ECD spectra of recombinant SM6 glycoforms produced in plants ($SM6_{wt}$, $SM6_{\Delta XF}$, and $SM6_{sia}$) and human cell lines ($SM6_{Per}$).

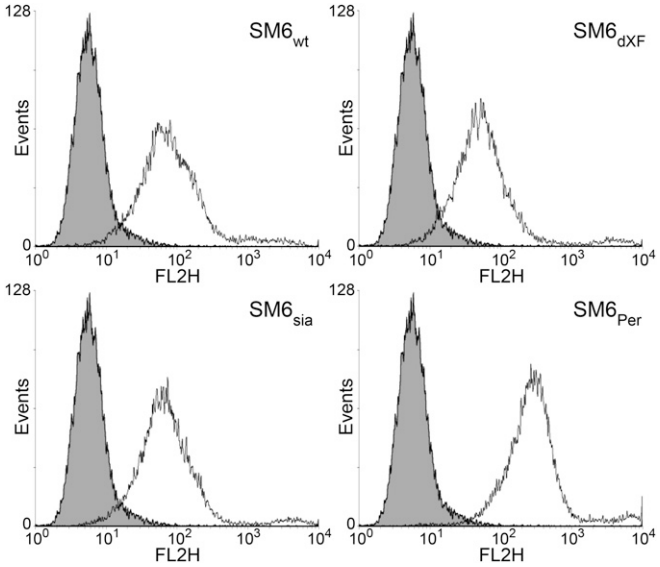

Fig. 5. Plant- and PER.C6-derived SM6 glycoforms exhibit similar antigen-binding properties. Different SM6 glycoforms produced in plants as well as in PER.C6 cells were tested for antigen binding by flow cytometry using human lung cancer cell line A549 as target. Here, 5 μg/mL SM6 (black curve) as well as 5 μg/mL unrelated control IgM (gray filled curve) were used with anti-human IgM PE as secondary antibody.

Discussion

This work presents the expression of the correctly folded and assembled IgM SM6 in plants. Plant-derived SM6 forms hexamers and pentamers, the major variants of circulating human-serum IgM. A difference to mammalian IgM is a significantly higher amount of hexamers in the plant-derived IgM. These findings indicate a reduced incorporation of the JC into plant-produced IgM, as this protein promotes pentamer formation (e.g., 29). Although it was shown previously that plant cells are able to produce complex mammalian proteins like IgGs and IgAs (reviewed by ref. 30), the correct assembly of a human molecule that consists of 21 or 24 subunits (pentamers or hexamers) with more than 50 glycans and over 100 disulfide bonds is remarkable. In mammalian plasma cells IgMs are produced and assembled in a multistep process that stretches along the secretory pathway and requires the action of various chaperons (such as Erp44, ERGIC57) and even specialized organelles (ERGIC) (7). Such components have so far not been identified in plants. At the moment it is unclear how plant cells handle such complex molecules, however, proper assembly of IgM to heteromultimeric forms indicates the presence of plant chaperones/components with similar functions as in mammalian cells.

Purification of recombinant pharmaceuticals is often a limiting factor in the production process and a major contributor to final costs of good. The one-step standard purification procedure we used here allowed the isolation of highly pure IgM oligomers. Such purified IgM facilitates rapid structure–function analyses and could serve as a suitable starting point for further purification steps in potential industrial applications. Small differences in secondary structure/conformation and antigen binding between plant-derived SM6 and $SM6_{PER}$, which have been found by ECD spectroscopy and flow cytometry, might be attributed to the different purification procedures (acid elution from protein A resin for plant-produced SM6 vs. neutral elution for $SM6_{PER}$).

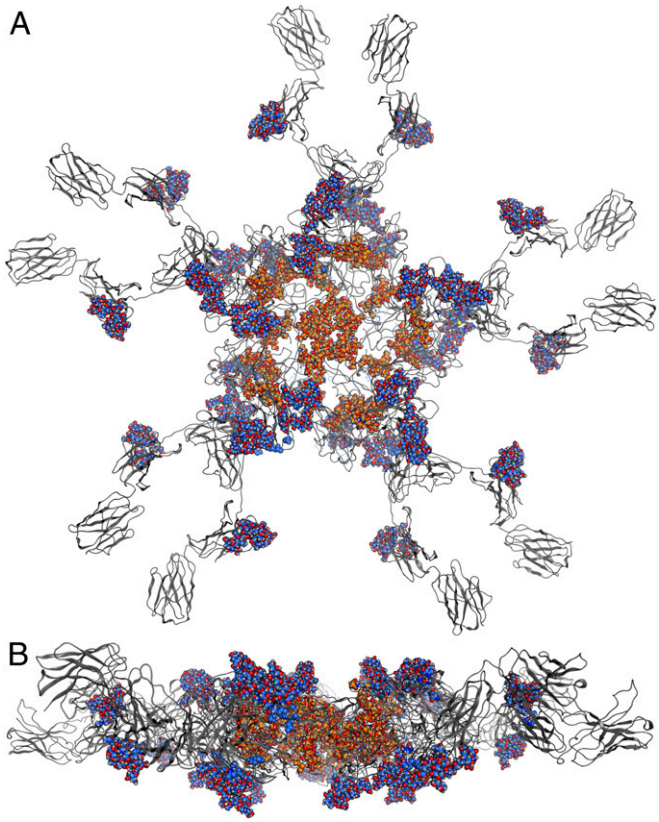

Fig. 6. Model of the heavy chain of SM6 including N-glycans. The protein is colored in gray, complex N-glycans (NaNa) are represented as blue/red space-filling models and the oligomannosidic glycans (Man8) as orange/red space-filling models. (*A*) Top view and (*B*) side view.

Interestingly, modified glycosylation does not seem to have an effect on the structural integrity as demonstrated by virtually identical ECD profiles.

Another important aspect of this work is the exact elucidation of the glycosylation status of human- and plant-derived SM6. Although site-specific differences in glycosylation have been proposed for human-serum IgM (22), to our knowledge experimental data showing the profiles of specific N-glycosylation sites of human-serum IgM were so far missing. Here, we confirmed the presence of complex, mainly sialylated carbohydrates on the N-terminally located GS1–3 and oligomannosidic structures on GS4 and GS5. The overall glycan composition was consistent with data shown previously (22). Notably, the glycosylation status of human-cell-line–produced $SM6_{PER}$ largely resembled that of serum IgM, with the main exception that the recombinant protein carried hardly any bisected structures. Plant-derived SM6 variants exhibited the same site-specific distribution of N-glycans as human-serum IgM and $SM6_{PER}$, mainly complex structures on GS1–3 and oligomannosidic ones on GS4 and GS5. It is important to note that the plant production system is amenable to glycoengineering, allowing the generation of variants with human-type glycosylation ($SM6_{\Delta XF}$, $SM6_{sia}$). Minor amounts of fucosylation in the ΔXT/FT glycomutant plant (e.g., GnGnF in $SM6_{\Delta XF}$) have been observed in previous studies and are probably due to incomplete silencing of the α1,3-fucosyltransferase responsible for this modification (24). Our results demonstrated the generation of additional IgM glycoforms using the plant-based glycoengineering platform developed in our laboratory (31). This will allow the investigation of the so-far-unexplored impact of glycosylation on the functioning of IgMs. In a first step, we show here antigen-binding properties that are virtually identical for the plant-derived SM6 glycoforms and similar to $SM6_{PER}$. This is not surprising because at least in IgGs glycosylation mainly influences Fc-based downstream effector functions (32).

Albeit known from other proteins, including IgE and IgD (9), the presence of complex and oligomannosidic N-glycans on a single protein is a peculiarity. To date, the biological relevance as well as the processes that drive this shift in glycosylation are poorly understood (33). The glycosylated model of pentameric IgM presented here explains altered glycosylation patterns as a consequence of different accessibility of the glycosylation sites. This is in accordance with previous results on a mouse IgM (27). Also other studies cite protein folding/assembly and inaccessibility to N-glycosylation enzymes as major reasons for the presence of oligomannosidic N-glycans on secreted proteins (26).

Overall, the generation of functionally active, multimeric IgMs in plants opens new ways for the expression of complex human proteins for therapeutic applications. Moreover, the possibility to efficiently produce different well-characterized IgM glycoforms provides practical tools to elucidate the impact of glycosylation on the biological properties of IgMs and thus may accelerate the generation of therapeutic proteins with optimized functions.

Experimental Procedures

Cloning. SM6 heavy and light chains (19, 20) were codon-optimized for *N. benthamiana* and cloned into Magnicon-based vectors pICHα31160 and pICHα26033, respectively (23). The codon-optimized joining chain (GenBank Accession NP_653247.1) lacking the 22-bp signal peptide was fused to the barley alfa amylase signal peptide and cloned into the binary vector pPT2 (34). HC- and LC-containing vectors were transformed into GV3101pMP90RK agrobacteria, the JC-containing vector into UIA143pMP90.

Agroinfiltration. Wild-type *N. benthamiana* plants as well as ΔXT/FT mutants (ref. 21; ΔXF) were infiltrated with Sam6HC, Sam6LC, and JC at OD_{600} of 0.01 each as previously described (12, 21). To achieve extension of both glycan arms, pGnTII (23) was coinfiltrated at an OD_{600} of 0.2. For production of sialylated IgM vectors expressing GNE, NANP, CMAS, CST, GalT, and α2,6-ST (24) were additionally infiltrated at an OD of 0.05.

Nonreducing Gels. The 3–12% native polyacrylamide gels, 4x NP LDS sample buffer and Nupage SDS running buffer were purchased from Life Technologies. IgM was precipitated with acetone at −20 °C for 1 h, resuspended in 1x NP LDS sample buffer and incubated for 30 min at RT before loading. Gels were run at 150 V for approximately 2 h and stained with Coomassie brilliant blue.

Purification and Quantification of SM6. Infiltrated leaf material was crushed in liquid nitrogen and extracted in 45 mM Tris, 1.5 M NaCl, 1 mM EDTA, 40 mM ascorbic acid, pH 7.4. Upon centrifugation (30 min, 4 °C, 30,000 × *g*), the supernatant was filtered (12–13 μm), centrifuged again and passed through a series of filters (12–13, 2–3, 0.45, and 0.2 μm). IgM was bound to protein A Sepharose (GE Healthcare, 17–1279-01) at 1 mL/min. The column was washed with 50 mM Hepes, 3 M sodium chloride, 200 mM arginine pH 7.0, and the IgM was eluted with 100 mM arginine, 100 mM NaAc, pH 3.0. The 3 mL fractions were collected and immediately neutralized with 1 M Tris, 1.5 M NaCl, pH 8.0. IgM-containing fractions were pooled, concentrated using ultrafiltration cartridges (Corning, 431484), and the buffer was exchanged to 12.2 mM Na_2HPO_4, 7.8 mM NaH_2PO_4, 55 mM arginine, 100 mM NaCl, pH 7.0 on PD-10 columns (GE Healthcare). Purified IgM was stored at 4 °C. Purification of $SM6_{PER}$ is described elsewhere (6, 24). Purified IgM was quantified via the BCA Protein Assay Kit using BSA as standard (Pierce, Thermo Scientific).

Glycan Analysis. The N-glycosylation profile of each SM6 glycosylation site was separately determined by LC-ESI-MS as previously published (35). In brief, purified IgM was separated by reducing SDS-PAGE, Coomassie stained, and the heavy chain band was excised from the gel. Upon S-alkylation and tryptic or tryptic/GluC digestion, fragments were eluted from the gel with 50% acetonitrile and separated on a Reversed Phase Column (150 × 0.32 mm BioBasic-18, Thermo Scientific) with a gradient of 1–80% acetonitrile. Glycopeptides were analyzed with a Q-TOF Ultima Global mass spectrometer (Waters). Spectra were summed and deconvoluted for identification of

glycoforms. Glycans were annotated according to the proglycan nomenclature (www.proglycan.com).

Antigen Binding. Binding of SM6 to tumor cell lines was assayed on an FACS (FACSCalibur, Becton & Dickinson) as described previously (5). In brief, the human-lung carcinoma cell line A549 was detached with enzyme-free detaching solution (Millipore), washed and incubated with 0, 5, or 25 μg/mL of SM6 or unrelated IgM (ChromPure IgM, Dianova). After 30 min incubation, cells were washed and incubated with PE-conjugated anti-human IgM antibody 1:50 diluted in PBS (donkey anti-human IgM-PE conjugated; Dianova) for 30 min. After washing, PE-staining was assessed by flow cytometry.

Size Exclusion Chromatography. Size exclusion chromatography (SEC) was performed on a Shimadzu LC20 HPLC system equipped with differential refractometric and UV/VIS photodiode array detector. Proteins were loaded onto a 5 μm 7.8 × 300 mm SEC Protein Column plus 7.8 × 5 mm guard column (WYATT Technology Corporation) at 25 °C and 0.5 mL/min isocratic flow with PBS containing 200 mM NaCl as running buffer. Elution was monitored by measuring the absorption at 280 nm. Standard was obtained from BioRad (151-1901).

Electronic Circular Dichroism (ECD) Spectroscopy. Experiments were performed using a Chirascan spectrometer (Applied Photophysics) that allowed simultaneous UV–vis and ECD monitoring and was equipped with a Peltier temperature control unit. The instrument was flushed with nitrogen with a flow rate of 3 L min^{-1}. For recording far-UV spectra (190–260 nm) the quartz cuvette had a path length of 1 mm. The spectral bandwidth was set to 3 nm; step size, 1 nm; scan time, 15 min; protein concentration, 0.15 mg/mL. All CD measurements were performed in PBS (140 mM NaCl, 2.7 mM KCl, 10 mM Na_2HPO_4, 2 mM KH_2PO_4, pH 7.4), at 25 °C. Each spectrum was automatically corrected with the base line to remove birefringence of the cell.

Modeling. A model of the heavy chain of IgM was made by constructing individual homology models for the five domains by using SWISS Model (36) in the automated mode. The following templates from the Brookhaven protein databank were used for the various domains: 3F12 for the VH domain, 2AGJ for the CH1 domain, 3QH3 for the CH2 domain, 2W59 for the CH3 domain, and 2QEJ for the CH4 domain. The orientation of these domains and the linkage between them were based on the model of Czajkowsky et al. (28), which was kindly provided to us by the authors. In PyMOL (1.2.r2) the backbone of the modeled domains were superimposed onto a monomer of the previously published IgM model. An energy minimization of the resulting structure was performed using the Groningen molecular simulation computer program package (GROMOS) 11 simulation package in conjunction with the GROMOS 54a7 force field (37) to remove any possible strain. The pentamer was subsequently constructed by superposition of the minimized structure onto the full model of Czajkowsky et al. (28). The molecular operating environment (MOE 2011.10) program was used to manually add glycans to the conserved N-glycosylation sites Asn171, Asn332, Asn395, Asn402, and Asn563. The complex N-glycan NaNa was added to Asn171, Asn332, and Asn395, and the oligomannosidic Man8 to Asn402 and Asn563. The full structure was finally energy minimized by using the force field AMBER99 (38) as implemented in the program MOE. The coordinates are available in Dataset S1.

ACKNOWLEDGMENTS. We thank Michaela Bogner and Thomas Hackl, Department of Applied Genetics and Cell Biology (University of Natural Resources and Life Sciences) for excellent technical support; Zhifeng Shao and Daniel Czajkowsky (University of Virginia) for making their IgM model available; and Deanne Greenwood (Patrys Limited) for critically reviewing this manuscript. This work was supported by the Austrian Research Promotion Agency Laura Bassi Centres of Expertise Grant 822757 (to H.S.), the Austrian Science Fund Grant L575-B13 (to H.S.), and the Vienna Science and Technology Fund Grant LS08-QM03 (to C.O.).

1. Vollmers HP, Brändlein S (2009) Natural antibodies and cancer. *New Biotechnol* 25(5): 294–298.
2. Vollmers HP, Brändlein S (2006) Natural IgM antibodies: The orphaned molecules in immune surveillance. *Adv Drug Deliv Rev* 58(5-6):755–765.
3. Horn MP, et al. (2010) Preclinical in vitro and in vivo characterization of the fully human monoclonal IgM antibody KBPA101 specific for Pseudomonas aeruginosa serotype IATS-O11. *Antimicrob Agents Chemother* 54(6):2338–2344.
4. Hensel F, Eckstein M, Rosenwald A, Brändlein S (2013) Early development of PAT-SM6 for the treatment of melanoma. *Melanoma Res* 23(4):264–275.
5. Tchoudakova A, et al. (2009) High level expression of functional human IgMs in human PER.C6 cells. *MAbs* 1(2):163–171.
6. Valasek C, et al. (2011) Production and purification of a PER.C6-expressed IgM antibody therapeutic. *BioProcess Int* 9(11):28–37.
7. Anelli T, et al. (2007) Sequential steps and checkpoints in the early exocytic compartment during secretory IgM biogenesis. *EMBO J* 26(19):4177–4188.
8. Zauner G, et al. (2013) Glycoproteomic analysis of antibodies. *Mol Cell Proteomics* 12(4):856–865.
9. Arnold JN, Wormald MR, Sim RB, Rudd PM, Dwek RA (2007) The impact of glycosylation on the biological function and structure of human immunoglobulins. *Annu Rev Immunol* 25(1):21–50.
10. Suzuki H, et al. (2008) IgA1-secreting cell lines from patients with IgA nephropathy produce aberrantly glycosylated IgA1. *J Clin Invest* 118(2):629–639.
11. Castilho A, Steinkellner H (2012) Glyco-engineering in plants to produce human-like N-glycan structures. *Biotechnol J* 7(9):1088–1098.
12. Giritch A, et al. (2006) Rapid high-yield expression of full-size IgG antibodies in plants coinfected with noncompeting viral vectors. *Proc Natl Acad Sci USA* 103(40): 14701–14706.
13. Hossler P, Khattak SF, Li ZJ (2009) Optimal and consistent protein glycosylation in mammalian cell culture. *Glycobiology* 19(9):936–949.
14. Loos A, Steinkellner H (2012) IgG-Fc glycoengineering in non-mammalian expression hosts. *Arch Biochem Biophys* 526(2):167–173.
15. Forthal DN, et al. (2010) Fc-glycosylation influences Fcγ receptor binding and cell-mediated anti-HIV activity of monoclonal antibody 2G12. *J Immunol* 185(11): 6876–6882.
16. Strasser R, et al. (2009) Improved virus neutralization by plant-produced anti-HIV antibodies with a homogeneous beta1,4-galactosylated N-glycan profile. *J Biol Chem* 284(31):20479–20485.
17. Shinkawa T, et al. (2003) The absence of fucose but not the presence of galactose or bisecting N-acetylglucosamine of human IgG1 complex-type oligosaccharides shows the critical role of enhancing antibody-dependent cellular cytotoxicity. *J Biol Chem* 278(5):3466–3473.
18. Kaneko Y, Nimmerjahn F, Ravetch JV (2006) Anti-inflammatory activity of immunoglobulin G resulting from Fc sialylation. *Science* 313(5787):670–673.
19. Pohle T, Brändlein S, Ruoff N, Müller-Hermelink HK, Vollmers HP (2004) Lipoptosis: Tumor-specific cell death by antibody-induced intracellular lipid accumulation. *Cancer Res* 64(11):3900–3906.
20. Brändlein S, et al. (2007) The human IgM antibody SAM-6 induces tumor-specific apoptosis with oxidized low-density lipoprotein. *Mol Cancer Ther* 6(1):326–333.
21. Strasser R, et al. (2008) Generation of glyco-engineered Nicotiana benthamiana for the production of monoclonal antibodies with a homogeneous human-like N-glycan structure. *Plant Biotechnol J* 6(4):392–402.
22. Arnold JN, et al. (2005) Human serum IgM glycosylation: Identification of glycoforms that can bind to mannan-binding lectin. *J Biol Chem* 280(32):29080–29087.
23. Schneider JD, et al. (2014) Expression of human butyrylcholinesterase with an engineered glycosylation profile resembling the plasma-derived orthologue. *Biotechnol J* 9(4):501–510.
24. Castilho A, et al. (2010) In planta protein sialylation through overexpression of the respective mammalian pathway. *J Biol Chem* 285(21):15923–15930.
25. Pabst M, Chang M, Stadlmann J, Altmann F (2012) Glycan profiles of the 27 N-glycosylation sites of the HIV envelope protein CN54gp140. *Biol Chem* 393(8):719–730.
26. Faye L, Sturm A, Bollini R, Vitale A, Chrispeels MJ (1986) The position of the oligosaccharide side-chains of phytohemagglutinin and their accessibility to glycosidases determines their subsequent processing in the Golgi. *Eur J Biochem* 158(3):655–661.
27. Cals M-M, et al. (1996) IgM polymerization inhibits the Golgi-mediated processing of the mu-chain carboxy-terminal glycans. *Mol Immunol* 33(1):15–24.
28. Czajkowsky DM, Shao Z (2009) The human IgM pentamer is a mushroom-shaped molecule with a flexural bias. *Proc Natl Acad Sci USA* 106(35):14960–14965.
29. Eskeland T, Christensen TB (1975) IgM molecules with and without J chain in serum and after purification, studied by ultracentrifugation, electrophoresis, and electron microscopy. *Scand J Immunol* 4(3):217–228.
30. De Muynck B, Navarre C, Boutry M (2010) Production of antibodies in plants: Status after twenty years. *Plant Biotechnol J* 8(5):529–563.
31. Bosch D, Castilho A, Loos A, Schots A, Steinkellner H (2013) N-glycosylation of plant-produced recombinant proteins. *Curr Pharm Des* 19(31):5503–5512.
32. Jefferis R (2009) Recombinant antibody therapeutics: The impact of glycosylation on mechanisms of action. *Trends Pharmacol Sci* 30(7):356–362.
33. Nagae M, Yamaguchi Y (2012) Function and 3D structure of the N-glycans on glycoproteins. *Int J Mol Sci* 13(7):8398–8429.
34. Strasser R, et al. (2005) Molecular basis of N-acetylglucosaminyltransferase I deficiency in Arabidopsis thaliana plants lacking complex N-glycans. *Biochem J* 387(Pt 2):385–391.
35. Stadlmann J, Pabst M, Kolarich D, Kunert R, Altmann F (2008) Analysis of immunoglobulin glycosylation by LC-ESI-MS of glycopeptides and oligosaccharides. *Proteomics* 8(14):2858–2871.
36. Arnold K, Bordoli L, Kopp J, Schwede T (2006) The SWISS-MODEL workspace: A web-based environment for protein structure homology modelling. *Bioinformatics* 22(2): 195–201.
37. Schmid N, et al. (2011) Definition and testing of the GROMOS force-field versions 54A7 and 54B7. *Eur Biophys J* 40(7):843–856.
38. Wang JM, Cieplak P, Kollman PA (2000) How well does a restrained electrostatic potential (RESP) model perform in calculating conformational energies of organic and biological molecules? *J Comput Chem* 21(12):1049–1074.